Cyclotron resonance phenomena in a non-neutral plasma

S. A. Prasad, G. J. Morales, and B. D. Fried
Department of Physics, University of California, Los Angeles, California 90024

(Received 29 December 1986; accepted 25 June 1987)

A kinetic theory of electrostatic cyclotron waves in a single component plasma slab of density $n_0(x)$ immersed in a uniform magnetic field $B_0\hat{z}$ is presented. The space charge electric field $E_0(x)\hat{x}$ in such a plasma modifies the single particle gyrofrequency from $\Omega = qB_0/mc$ to $\Omega_1(x) = [\Omega^2 - \omega_p^2(x)]^{1/2}$ in the limit $r_c/L \ll 1$ (where r_c is the orbit size and $L^{-1} = d \ln E_0/dx$), causing the upper hybrid frequency to have the value $(\Omega_1^2 + \omega_p^2)^{1/2} = \Omega$. Finite Larmor radius effects introduce a velocity dependence into the single particle gyrofrequency Ω_1, leading to energy transfer to the particles located at the resonant layers where $\omega - k_y v_E(x) = \Omega_1(x)$ [$v_E(x)\hat{y}$ being the $\mathbf{E}\times\mathbf{B}$ drift velocity]. This energy transfer mechanism is operative even when $k_z = 0$. Another nonzero Larmor radius effect is the appearance of thermal modes that are the analogs of Bernstein modes of neutral plasmas. When driven by an external capacitor plate antenna, these modes exhibit behavior similar to Tonks–Dattner resonances.

I. INTRODUCTION

The description of wave propagation in nonuniform plasmas is a central theme in several areas of current plasma research, such as rf heating of fusion plasmas, collective transport, and drift instabilities. In conventional neutral plasmas, the nonuniformity is usually associated with density, temperature, and the confining magnetic field. One other possible source of nonuniformity is the presence of zeroth-order electrostatic fields,[1] e.g., ambipolar fields arising from the different transport rates of electrons and ions. In order to highlight the effect of electric field nonuniformity on the propagation of waves, the present study considers the extreme case of a single component (i.e., fully non-neutral) plasma[2,3] confined by a uniform, straight magnetic field, with attention focused on the plasma response to wave frequencies near the vacuum cyclotron frequency Ω. The equilibrium static electric field is produced by the plasma itself and is related to the zeroth-order plasma density through Poisson's equation; the nonuniformities in the equilibrium electric field and density are thus not independent.

From the experimental point of view, single component plasmas exhibit remarkably long confinement times[4] in addition to being very quiescent as compared to most laboratory plasmas. Many theories, including the present one, whose motivation is to provide a better understanding of conventional neutral plasmas, can therefore be verified in this somewhat novel environment to a degree not attainable in other plasmas.

Wave propagation in a magnetized nonuniform nonneutral plasma is primarily governed by two scale length parameters. The first one, the ratio of the single particle orbit size (Larmor radius) r_c to the wave field scale length k^{-1} (perpendicular to the magnetic field) is a measure of the variation of the oscillating wave electric field across the Larmor orbit. As in neutral plasmas, the value of this parameter determines the appropriate mathematical description (integrodifferential or differential) of the problem. The second parameter, the ratio of r_c to the scale length L of the nonuniformity, is related to the effect of the equilibrium static electric field on the zeroth-order orbit of a particle. The zeroth-order (or unperturbed) particle orbit, which determines the single particle properties (such as gyrofrequency, drifts, etc.) entering into the plasma kinetic response, can in general be obtained analytically only for small values of r_c/L, and then as a power series expansion, with higher-order terms being corrections resulting from the nonuniformity of the static electric field across the particle orbit.

The present study concentrates on wave phenomena associated with small values of kr_c and hence the description is in terms of a finite-order differential equation derived systematically from the exact integrodifferential equation for the system. In addition, a truncated series in powers of r_c/L for the zeroth-order particle orbit is used to illustrate the finite Larmor radius single particle effects on the plasma response. The most important among these is the fact that the gyrofrequency of a particle becomes position dependent although the confining magnetic field is strictly uniform.

For the geometry considered in this paper, namely, a slab plasma (Fig. 1), whose density $n_0(x)$ varies in the x

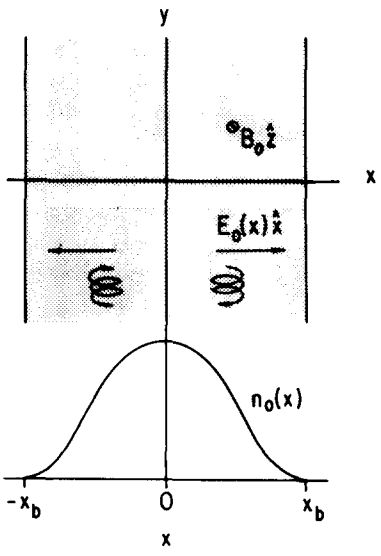

FIG. 1. The geometry. The straight arrows indicate the direction of the equilibrium self-electric field in the single component plasma slab and spirals represent orbits of typical plasma particles.

 0031-9171/87/103093-13$01.90

direction perpendicular to a strong, uniform confining magnetic field $\mathbf{B} = B_0\hat{z}$, a particle gyrates about its guiding center (at coordinate x) with an angular frequency $\Omega_1 = [\Omega^2 - \omega_p^2(x)]^{1/2}$, where $\Omega = qB_0/mc$ and $\omega_p = [4\pi q^2 n_0(x)/m]^{1/2}$ is the plasma frequency. This behavior can be readily understood by considering the x motion of the particle. In the absence of the electric field (as in a neutral plasma), the magnetic field provides a linear restoring force $-\Omega^2\delta$ (corresponding to a quadratic potential well in the displacement variable δ), which causes the particle to oscillate at frequency Ω. For small values of r_c/L, the effect of the nonuniform self-electric field can be obtained by using its Taylor expansion about the guiding center position x. The leading contribution $qE_0(x)/m$ to the expression for the acceleration $\ddot{\delta}$ gives rise to a drift in the y direction while the linear term $qE_0'(x)\delta/m = \omega_p^2(x)\delta$ [using Poisson's equation] weakens the magnetic restoring force and hence modifies the oscillation frequency from Ω to $\Omega_1 = [\Omega^2 - \omega_p^2(x)]^{1/2}$. Thus the fact that the electric field is generated by the plasma itself causes the appearance of a collective feature ω_p in the single particle property Ω_1.

An immediate consequence of a single particle gyrating at frequency $\Omega_1(x)$ rather than the usual value Ω for neutral plasmas is that the familiar roles of particle resonance and collective resonance become in a sense interchanged in single component slab plasmas. A review of how these resonances appear in the plasma response makes this clear. In a cold magnetized neutral plasma, the cross-field behavior for frequency ω near Ω is determined by the dielectric tensor element $\epsilon_{xx} = 1 - \omega_p^2/(\omega^2 - \Omega^2) = (\omega^2 - \omega_{uh}^2)/(\omega^2 - \Omega^2)$, where the upper hybrid frequency ω_{uh} is defined by $\omega_{uh} = (\Omega^2 + \omega_p^2)^{1/2}$. Thus, $\epsilon_{xx} \to \infty$ at the single particle resonance $\omega = \Omega$ and $\epsilon_{xx} \to 0$ at the collective resonance $\omega = \omega_{uh}$. For a neutral plasma slab having the geometry shown in Fig. 1, the application of an external capacitor plate field $E_c \exp(-i\omega t)\hat{x}$ results in a plasma electric field $E_1 = E_c/\epsilon_{xx}$, which vanishes for all x when $\omega = \Omega$ and has a local singularity at layers where $\omega = \omega_{uh}(x)$.

In a single component plasma, however, the single particle gyrofrequency is $\Omega_1 = (\Omega^2 - \omega_p^2)^{1/2}$ and the corresponding cold plasma dielectric tensor element ϵ_{xx} is given by $\epsilon_{xx} = 1 - \omega_p^2/(\omega^2 - \Omega_1^2) = (\omega^2 - \Omega^2)/(\omega^2 - \Omega_1^2)$. Consequently, $\epsilon_{xx} \to 0$ as $\omega \to \Omega$ and $\epsilon_{xx} \to \infty$ as $\omega \to \Omega_1$. In a slab driven by a capacitor field, the plasma electric field $E_1 = E_c/\epsilon_{xx}$ vanishes locally at layers where $\omega = \Omega_1(x)$ and has a global singularity when $\omega = \Omega$. It should be noted that the upper hybrid frequency $\omega_{uh} = (\Omega_1^2 + \omega_p^2)^{1/2}$ is spatially constant (and equal to Ω) only for a completely non-neutral system. For a fractionally neutralized system, ω_{uh} is position dependent and the singularity of the electric field is localized to layers where $\omega = \omega_{uh}(x)$.

The inclusion of finite temperature effects modifies the nulls and singularities in the response of a single component plasma slab to an external driver. In what follows, the assumption $k_z = 0$ is made and the effect of nonzero k_z, which is straightforward to include, is only briefly indicated. Thus the finite temperature effects considered here are basically those connected with nonzero perpendicular temperature. There are two such finite Larmor radius effects. The first one is the appearance of thermal modes that are the analogs of Bernstein modes found in neutral plasmas. The differential equation developed for the system describes the cold plasma response in the lowest order in kr_c. For a capacitor plate antenna, this response (discussed earlier) does not have wavelike behavior, while an antenna with $k_y \neq 0$ does give rise to a wavelike response for frequencies near Ω (upper hybrid mode), as well as for low frequencies on the order of $k_y v_E(x)$ (diocotron mode), where $v_E(x)$ is the velocity of the $\mathbf{E}\times\mathbf{B}$ drift of the plasma caused by the equilibrium static electric field. Successively higher-order thermal corrections obtained by retaining higher-order terms (in powers of kr_c) in the differential equation describe wave phenomena near higher harmonics of the gyrofrequency Ω_1.

The second finite Larmor radius effect is one that provides a mechanism for the gyrating particles to absorb energy from the waves at the resonant layers where the frequency $\omega - k_y v_E(x)$ (Doppler-shifted because of the zeroth-order $\mathbf{E}\times\mathbf{B}$ drift) matches the gyrofrequency $\Omega_1(x)$ or its harmonics. To understand this, it is helpful to return to the potential well description of the motion of the particle. As described earlier, the linear term in the Taylor expansion of the electric field weakens the magnetic restoring force and causes the particle to oscillate at a frequency Ω_1. Inclusion of quadratic and higher-order terms causes the oscillation frequency to become velocity dependent since the potential well is no longer parabolic (or even symmetric). A Maxwellian velocity distribution of particles gives rise to a corresponding distribution of gyrofrequencies; hence the resonant denominators in the differential equation are replaced by the appropriate plasma dispersion functions indicating absorption of wave energy by resonant particles.[5] The physical mechanism for energy absorption is similar to the familar cyclotron damping (even though in the present system $k_z = 0$).

The paper is organized as follows. The linear Vlasov equation describing electrostatic waves in a single species plasma slab is formally solved in Sec. II. The solution, when introduced into the linearized Poisson equation, yields an integrodifferential equation, which is systematically expanded in the limit of small kr_c into an infinite-order differential equation involving expressions for the orbit of a single particle in the equilibrium electric and magnetic fields. These orbits are obtained in Sec. III, as an expansion in powers of r_c/L (where L is the scale length of variation of the equilibrium static electric field) using secular perturbation theory. A Vlasov equilibrium distribution function $f_0(\mathbf{r},\mathbf{v})$, which describes a single species plasma slab such as the one shown in Fig. 1, is constructed in Sec. IV and density profiles consistent with the self-electric fields are derived. The distribution f_0 and the orbits in the corresponding electric field (and the external magnetic field) are used to find the plasma response in Secs. V and VI. Section V describes the cold plasma response for the cases $k_y = 0$ and $k_y \neq 0$. The effects of finite temperature are discussed in Sec. VI for these cases. Finite temperature effects include finite kr_c effects which give rise to thermal modes analogous to Bernstein modes found in neutral plasmas and finite r_c/L effects which give rise to transfer of energy from the wave fields to resonant particles.

II. KINETIC FORMULATION

The linearized Vlasov equation for electrostatic modes in a single component plasma slab (Fig. 1) propagating perpendicular to the uniform constant external magnetic field $B_0\hat{z}$ is

$$\frac{\partial f_1}{\partial t}+\mathbf{v}\cdot\frac{\partial f_1}{\partial \mathbf{r}}+\left(\frac{q}{m}\mathbf{E}_0(x)\hat{x}+\Omega\mathbf{v}\times\hat{z}\right)\cdot\frac{\partial f_1}{\partial \mathbf{v}} = -\frac{q}{m}\mathbf{E}_1\cdot\frac{\partial f_0}{\partial \mathbf{v}}, \tag{1}$$

where $\mathbf{r}$ and $\mathbf{v}$ denote position and velocity in the xy plane. Also, q and m are the charge and the mass, respectively, of a plasma particle, $\Omega = qB_0/mc$ is the vacuum cyclotron frequency, $f_0(x,y)$ the equilibrium distribution function that self-consistently produces the electric field $E_0(x)\hat{x}$, $f_1(\mathbf{r},\mathbf{v})$ the perturbed distribution function, and $\mathbf{E}_1$ the corresponding perturbed electric field.

The Green's function solution to Eq. (1) is

$$f_1(\mathbf{r},\mathbf{v},t) = \int dt_0\, d\mathbf{r}_0\, d\mathbf{v}_0\, \delta[\mathbf{r}-\mathbf{R}(t-t_0,\mathbf{r}_0,\mathbf{v}_0)] \times\delta[\mathbf{v}-\mathbf{V}(t-t_0,\mathbf{r}_0,\mathbf{v}_0)]\theta(t-t_0) \times\left(-\frac{q}{m}\mathbf{E}_1(\mathbf{r}_0,t_0)\cdot\frac{\partial f(x_0,\mathbf{v}_0)}{\partial \mathbf{v}_0}\right), \tag{2}$$

where $\theta(t-t_0)$ is the Heaviside step function and $\mathbf{R}$ and $\mathbf{V}$ are the position and velocity at time t of a particle moving under the influence of the unperturbed fields $E_0(x)\hat{x}$ and $B_0\hat{z}$, starting at time t_0 with position $\mathbf{r}_0$ and velocity $\mathbf{v}_0$. The vectors $\mathbf{R}$ and $\mathbf{V}$ satisfy the equations

$$\frac{d\mathbf{V}}{dt}=\frac{q}{m}E_0(X)\hat{x}+\Omega\mathbf{V}\times\hat{z}, \tag{3a}$$

$$\frac{d\mathbf{R}}{dt}=\mathbf{V}, \tag{3b}$$

$$\mathbf{V}(0,\mathbf{r}_0,\mathbf{v}_0)=\mathbf{v}_0, \tag{3c}$$

$$\mathbf{R}(0,\mathbf{r}_0,\mathbf{v}_0)=\mathbf{r}_0. \tag{3d}$$

The perturbed density $n_1(\mathbf{r},t)$ is obtained by integrating f_1 over velocity [making use of the delta function $\delta(v-V)$]:

$$n_1(\mathbf{r},t) = -\frac{q}{m}\int_{-\infty}^{t} dt_0\, d\mathbf{r}_0\, d\mathbf{v}_0\, \delta[\mathbf{r}-\mathbf{R}(t-t_0,\mathbf{r}_0,\mathbf{v}_0)] \times\mathbf{E}_1(\mathbf{r}_0,t_0)\cdot\frac{\partial f_0(x_0,\mathbf{v}_0)}{\partial \mathbf{v}_0}. \tag{4}$$

Since the equilibrium is translationally invariant in y, the perturbed quantities can be Fourier analyzed in y and each Fourier component treated separately. Therefore, the perturbed density and the electric field at frequency ω can be assumed to be of the form

$$n_1(\mathbf{r},t) = n_1(x)\exp[i(k_y y-\omega t)], \tag{5a}$$

$$\mathbf{E}_1(\mathbf{r},t) = -\nabla\{\phi_1(x)\exp[i(k_y y-\omega t)]\}, \tag{5b}$$

where $\phi_1(x)$ is the x-dependent part of the perturbed complex potential. Inserting Eqs. (5a) and (5b) in Eq. (4) and replacing t_0-t by τ results in

$$n_1(x) = \frac{q}{m}\int_{-\infty}^{0} d\tau\, e^{-i\omega\tau}\int d\mathbf{r}_0\, d\mathbf{v}_0\, \delta[\mathbf{r}-\mathbf{R}(-\tau,\mathbf{r}_0,\mathbf{v}_0)] \times\left(\frac{d\phi_1(x_0)}{dx_0}\hat{x}+ik_y\phi_1(x_0)\hat{y}\right) \cdot\frac{\partial f_0(x_0,\mathbf{v}_0)}{\partial \mathbf{v}_0}\exp[ik_y(y_0-y)]. \tag{6}$$

Since the system in equilibrium is translationally invariant in y, the particle orbit $\mathbf{R}$ can be expressed as

$$\begin{aligned}\mathbf{R}(-\tau,\mathbf{r}_0,\mathbf{v}_0) &= X(-\tau,x_0,\mathbf{v}_0)\hat{x}+[y_0-\tilde{Y}(-\tau,x_0,\mathbf{v}_0)]\hat{y}\\ &= X(-\tau,x_0,\mathbf{v}_0)\hat{x}+[y_0-v_d(x_0,\mathbf{v}_0)\tau\\ &\quad+\tilde{\tilde{Y}}(-\tau,x_0,\mathbf{v}_0)]\hat{y},\end{aligned} \tag{7}$$

where v_d is the $\mathbf{E}_0\times\mathbf{B}$ drift along $\hat{y}$ and the oscillatory quantities X and $\tilde{\tilde{Y}}$ satisfy the initial conditions $X(\tau=0)=x_0$ and $\tilde{\tilde{Y}}(\tau=0)=0$. Using Eq. (7), the integration over y_0 in Eq. (6) yields

$$n_1(x) = \frac{q}{m}\int_{-\infty}^{0} d\tau\, e^{-i\omega\tau}\int dx_0\, d\mathbf{v}_0 \times\left(\frac{d\phi_1(x_0)}{dx_0}\hat{x}+ik_y\phi_1(x_0)\hat{y}\right)\cdot\frac{\partial}{\partial \mathbf{v}_0}f_0(x_0,\mathbf{v}_0) \times\exp[-ik_y\tilde{Y}(-\tau,x_0,\mathbf{v}_0)] \times\delta[x-X(-\tau,\mathbf{x}_0,\mathbf{v}_0)]. \tag{8}$$

Substitution of Eq. (8) in the linearized Poisson equation results in an integrodifferential equation for ϕ_1. A differential equation for ϕ_1, which is useful for small values of kr_c, can also be obtained by expanding the delta function in Eq. (8) in a Taylor series about $X=x_0$:

$$\delta[x-X(-\tau,x_0,\mathbf{v}_0)] = \sum_{p=0}^{\infty}\frac{[x_0-X(-\tau,x_0,\mathbf{v}_0)]^p}{p!}\frac{\partial^p}{\partial x^p}\delta(x-x_0). \tag{9}$$

Substituting Eq. (9) in Eq. (8), the operator $\partial^p/\partial x^p$ can be moved outside of the integral symbols since none of the intervening factors depends on x. The integration over x_0 can then be performed using the delta function $\delta(x-x_0)$ and the dummy integration variable $\mathbf{v}_0$ replaced by $\mathbf{v}$ to yield the differential equation for ϕ_1:

$$\begin{aligned}\frac{d^2\phi_1}{dx^2}-k_y^2\phi_1 &= -4\pi q n_1(x)\\ &= -\frac{4\pi q^2}{m}\sum_{p=0}^{\infty}\frac{1}{p!}\frac{d^p}{dx^p}\int d\mathbf{v}\\ &\quad\times\left(\frac{d\phi_1}{dx}\frac{\partial}{\partial v_x}+ik_y\phi_1\frac{\partial}{\partial v_y}\right)f_0(x,\mathbf{v})\\ &\quad\times\int_{-\infty}^{0} d\tau\, e^{-i\omega\tau}[x-X(-\tau,x,\mathbf{v})]^p\\ &\quad\times\exp[-ik_y\tilde{Y}(-\tau,x,\mathbf{v})],\end{aligned} \tag{10}$$

where the integrals over velocity and time can be performed once the equilibrium distribution $f_0(x,\mathbf{v})$ is specified and the orbits in the corresponding zeroth-order fields [i.e., $\mathbf{E}_0(x)$ and $\mathbf{B}$] calculated.

Since $d\phi_1/dx \sim O(k_x\phi_1)$ and $x-X\sim O(r_c)$, the right-hand side of Eq. (10) is in a sense an expansion in powers of

$k_x r_c$. However, the derivatives with respect to x also apply to the equilibrium quantities and hence the nonlocal character of the plasma response is preserved in this description. Since $k_y \tilde{\tilde{Y}} \sim O(k_y r_c)$, the exponential in Eq. (10) (which is valid for arbitrary k_y) can be expanded to yield an equation useful in the limit of small $k_x r_c$ and $k_y r_c$:

$$\frac{d^2\phi_1}{dx^2} - k_y^2\phi_1 = -\frac{4\pi q^2}{m}\sum_{p=0}^{\infty}\frac{1}{p!}\frac{d^p}{dx^p}\int d\mathbf{v} \times\left(\frac{d\phi_1}{dx}\frac{\partial}{\partial v_x} + ik_y\phi_1\frac{\partial}{\partial v_y}\right) f_0(x,\mathbf{v}) \times\int_{-\infty}^{0} d\tau\, e^{-i\omega_1\tau}[x - X(-t,x,\mathbf{v})]^p \times\sum_{r=0}^{\infty}\frac{1}{r!}[-ik_y\tilde{\tilde{Y}}(-\tau,x,\mathbf{v})]^r, \tag{11}$$

where ω_1 is the Doppler-shifted frequency

$$\omega_1 = \omega - k_y v_d(x,\mathbf{v}). \tag{12}$$

It should be noted that Eqs. (10) and (11) are general results, valid also for a neutral plasma slab provided that a sum over all species is performed.[6]

To proceed further with Eq. (11) for a single component plasma slab, the equilibrium distribution function $f_0(x,\mathbf{v})$ and the single particle orbit in the corresponding self-electric field must be known. In the following section, the orbit in an electric field $E_0(x)\hat{x}$ [produced by an arbitrary density profile $n_0(x)$ such that $dE_0/dx = 4\pi q n_0(x)$] and magnetic field $B_0\hat{z}$ is calculated in terms of an expansion in the small parameter r_c/L. The requirement that $E_0(x)$ and $n_0(x)$ correspond to a Vlasov equilibrium limits them to certain specific forms which will be derived in Sec. IV for a suitable choice of f_0.

III. EQUILIBRIUM SINGLE PARTICLE ORBIT

A particle with charge q and mass m moving in the equilibrium self-electric field $E_0(x)\hat{x}$ and magnetic field $B_0\hat{z}$ satisfies the equation

$$\ddot{\mathbf{R}} = (q/m)E_0(X)\hat{x} + \Omega\dot{\mathbf{R}}\times\hat{z}, \tag{13}$$

where $\mathbf{R}(t,\mathbf{x},\mathbf{v})$ is the position vector of the particle at time t, starting with the initial conditions $\mathbf{R}(0,\mathbf{x},\mathbf{v}) = \mathbf{x}$ and $\dot{\mathbf{R}}(0,\mathbf{x},\mathbf{v}) = \mathbf{v}$ with a dot representing a derivative with respect to t and $\Omega = qB_0/mc$. The y component of Eq. (13) can be integrated subject to the initial conditions to yield

$$\dot{Y} = \Omega(x - X) + v_y. \tag{14}$$

Substituting this result in the x component of Eq. (13) gives

$$\ddot{X} = (q/m)E(X) - \Omega^2(x - X) + \Omega v_y = -\frac{\partial V(X)}{\partial X}, \tag{15}$$

where V is the effective potential for the x motion of the particle. This potential is an extremum for $X = X_m$ where $\partial V/\partial X$ vanishes, i.e.,

$$(q/m)E_0(X_m) + \Omega^2(x - X_m) + \Omega v_y = 0. \tag{16}$$

Equation (16) (which is, in general, transcendental) can be solved iteratively for X_m to yield

$$X_m = x + \frac{\Omega u_y}{\Omega_1^2} + \frac{1}{2\Omega_1^2}\frac{d\omega_p^2}{dx}\left(\frac{\Omega u_y}{\Omega_1^2}\right)^2 + \frac{1}{\Omega_1^2}\left[\frac{1}{6}\frac{d^2\omega_p^2}{dx^2} + \frac{1}{2\Omega_1^2}\left(\frac{d\omega_p^2}{dx}\right)^2\right]\left(\frac{\Omega u_y}{\Omega_1^2}\right)^3, \tag{17}$$

where

$$u_y = v_y + (1/\Omega)(q/m)E_0(x) \tag{18}$$

and

$$\Omega_1^2(x) = \Omega^2 - \frac{q}{m}\frac{dE_0(x)}{dx} = \Omega^2 - \omega_p^2(x). \tag{19}$$

Since

$$\left.\frac{\partial^2 V}{\partial X^2}\right|_{X=X_m} = \Omega^2 - \omega_p^2(X_m) > 0$$

for a strongly magnetized system, the effective potential V has a minimum at $X = X_m$ and the particle executes oscillations in a confining potential well.

The orbit of the particle is obtained by solving Eq. (15) in a perturbation series with r_c/L as the small expansion parameter and using the solution X in Eq. (14) to obtain Y. This procedure is carried out here to obtain the lowest finite Larmor radius corrections to the orbit. Introducing the dimensionless variable $\zeta = (X - X_m)/r_c$ (where $r_c = \bar{v}/\Omega$ is the typical size of an orbit), Eqs. (15) and (16) yield

$$\ddot{\zeta} + \nu^2\zeta = [\nu^2 - \Omega_1^2(X_m)]\zeta + \frac{r_c}{2}\left.\frac{d\omega_p^2(x)}{dx}\right|_{x=X_m}\zeta^2 + \frac{r_c^2}{6}\left.\frac{d^2\omega_p^2(x)}{dx^2}\right|_{x=X_m}\zeta^3 + \cdots, \tag{20}$$

where we have added ν^2 to both sides of the equation. Equation (20) is now in a form suitable for solving by the secular perturbation method,[7] which starts with the ansatz

$$\zeta = \zeta_0 + \zeta_1 + \cdots, \tag{21}$$

where

$$\zeta_0 = A_0\cos(\nu t + \theta_0), \tag{22}$$

$$\nu = \nu_0 + \nu_1 + \cdots, \tag{23}$$

and r_c/L is the small parameter of expansion. Equations (21)–(23) are substituted in Eq. (20) and coefficients of various powers of r_c/L are compared. The result in the zeroth order is

$$\nu_0 = \Omega_1(X_m) \simeq \Omega_1(x) - \frac{1}{2\Omega_1}\frac{d\omega_p^2}{dx}\frac{\Omega u_y}{\Omega_1^2}, \tag{24}$$

making use of Eq. (17). The first term on the right-hand side, $\Omega_1(x)$, is the single particle gyration frequency in the zero Larmor radius limit (with the equilibrium self-electric field being the cause for the position-dependent modification from the usual value Ω) while the second term represents the lowest finite Larmor radius correction to the gyration frequency.

In the first order, Eq. (20) yields

$$\ddot{\zeta}_1 + \nu^2\zeta_1 = 2\nu_0\nu_1\zeta_0 + \frac{r_c}{2}\frac{d\omega_p^2}{dX_m}\zeta_0^2, \tag{25}$$

with ζ_0 given by Eq. (22). To prevent a spurious secular growth of ζ_1, the terms on the right-hand side are not allowed to contain terms with frequency ν, implying

$$\nu_1 = 0. \tag{26}$$

Equation (25) can then be solved for ζ_1 yielding

$$\zeta_1 = \frac{1}{4}\frac{d\omega_p^2}{dX_m} r_c A_0^2 \left(\frac{1}{\nu^2} - \frac{1}{3\nu^2}\cos 2(\nu t + \theta_0)\right) \tag{27}$$

as the lowest-order finite Larmor radius correction to ζ.

The parameters A_0 and θ_0 appearing in Eqs. (22) and (27) are found by imposing the initial conditions

$$x - X_m = r_c\zeta(t=0) = r_c A_0 \cos\theta_0 + \frac{1}{4\nu^2}\frac{d\omega_p^2}{dX_m}(r_c A_0)^2 \times (1 - \tfrac{1}{3}\cos 2\theta_0), \tag{28}$$

$$v_x = r_c\dot{\zeta}(t=0) = -\nu r_c A_0 \sin\theta_0 + \frac{1}{6\nu}\frac{d\omega_p^2}{dX_m}(r_c A_0)^2 \sin 2\theta_0. \tag{29}$$

Equations (28) and (29) can be solved for $A_0\cos\theta_0$ and $A_0\sin\theta_0$ as expansions in r_c/L and the particle trajectory is thus determined in terms of its initial position r and velocity v. Replacing t by $-\tau$ to be consistent with the notation of Sec. II and including only the lowest-order finite Larmor radius corrections, it is found that

$$\begin{aligned} x - X(-\tau,x,\mathbf{v}) = &-\frac{\Omega}{\Omega_1^2}u_y - \frac{1}{\Omega_1^4}\frac{d\omega_p^2}{dx}\left(\frac{3}{4}\frac{\Omega^2}{\Omega_1^2}u_y^2 + \frac{1}{4}v_x^2\right) + \cos\nu\tau\left[\frac{\Omega}{\Omega_1^2}u_y + \frac{1}{\Omega_1^4}\frac{d\omega_p^2}{dx}\left(\frac{2}{3}\frac{\Omega^2}{\Omega_1^2}u_y^2 + \frac{1}{3}v_x^2\right)\right] \\ &+ \sin\nu\tau\left[\frac{v_x}{\Omega_1}\left(1 + \frac{\Omega}{6\Omega_1^4}\frac{d\omega_p^2}{dx}u_y\right)\right] + \cos 2\nu\tau\left[\frac{1}{12\Omega_1^4}\frac{d\omega_p^2}{dx}\left(\frac{\Omega^2}{\Omega_1^2}u_y^2 - v_x^2\right)\right] \\ &+ \sin 2\nu\tau\left(\frac{\Omega}{6\Omega_1^5}\frac{d\omega_p^2}{dx}u_y v_x\right), \end{aligned} \tag{30}$$

where

$$\nu = \Omega_1(x) - \frac{\Omega}{2\Omega_1^3}\frac{d\omega_p^2}{dx}u_y \simeq \Omega_1(X_m). \tag{31}$$

Equations (14) and (30) yield

$$Y(-\tau,\mathbf{x},\mathbf{v}) = y - \tilde{Y}(-\tau,x,\mathbf{v}) = y - v_d(x,\mathbf{v})\tau + \tilde{\tilde{Y}}(-\tau,x,\mathbf{v}), \tag{32}$$

where

$$\begin{aligned} \tilde{\tilde{Y}}(-\tau,x,\mathbf{v}) = &-\frac{\Omega}{\Omega_1}\sin\nu\tau\left[\frac{\Omega}{\Omega_1^2}u_y + \frac{1}{\Omega_1^4}\frac{d\omega_p^2}{dx}\left(\frac{7}{6}\frac{\Omega^2}{\Omega_1^2}u_y^2 + \frac{1}{3}v_x^2\right)\right] + \frac{\Omega}{\Omega_1}(\cos\nu\tau - 1) \\ &\times\left[\frac{v_x}{\Omega_1}\left(1 + \frac{2}{3\Omega_1^3}\frac{d\omega_p^2}{dx}\frac{\Omega u_y}{\Omega_1}\right)\right] - \frac{\Omega}{24\Omega_1}\sin 2\nu\tau\left[\frac{1}{\Omega_1^4}\frac{d\omega_p^2}{dx}\left(\frac{\Omega^2 u_y^2}{\Omega_1^2} - v_x^2\right)\right] \\ &+ \frac{\Omega}{12\Omega_1}(\cos 2\nu\tau - 1)\left[\frac{v_x}{\Omega_1}\left(\frac{1}{\Omega_1^3}\frac{d\omega_p^2}{dx}\frac{\Omega u_y}{\Omega_1}\right)\right], \end{aligned} \tag{33}$$

and the particle drift v_d along the y direction is

$$v_d(x,\mathbf{v}) = v_E(x) - (\omega_p^2/\Omega_1^2)u_y \simeq v_E(X_m). \tag{34}$$

In evaluating the integrals in Eqs. (10) and (11), it is also useful to derive exact relations between the partial derivatives of $X(-\tau,x,\mathbf{v})$ and $\tilde{Y}(-\tau,x,\mathbf{v})$. Such relations can be obtained by shifting the initial time by an infinitesimal amount Δ and calculating the corresponding changes in the initial conditions from Eq. (13). Thus

$$X(-\tau,x,v_x,v_y) = X(-\tau-\Delta,x+v_x\Delta,v_x + \Omega u_y\Delta,v_y - \Delta v_x\Delta) + O(\Delta^2)$$

and

$$\begin{aligned} Y(-\tau,\mathbf{x},\mathbf{v}) &= y + \tilde{Y}(-\tau,x,v_x,v_y) \\ &= y + v_y\Delta + \tilde{Y}(-\tau-\Delta,x+v_x\Delta,v_x + \Omega u_y\Delta,v_y - \Delta v_x\Delta) + O(\Delta^2), \end{aligned}$$

yielding

$$\frac{\partial X}{\partial\tau} + v_x\frac{\partial X}{\partial x} + \Omega u_y\frac{\partial X}{\partial v_x} - \Omega v_x\frac{\partial X}{\partial v_y} = 0 \tag{35a}$$

and

$$v_y + \frac{\partial\tilde{Y}}{\partial\tau} + v_x\frac{\partial\tilde{Y}}{\partial x} + \Omega u_y\frac{\partial\tilde{Y}}{\partial v_x} - \Omega v_x\frac{\partial\tilde{Y}}{\partial v_y} = 0. \tag{35b}$$

The approximate expressions derived in this section for X and $\tilde{Y}$ [Eqs. (30)–(34)] have a very complicated dependence on their arguments, but satisfy the rather simple (and exact) relations (35). These relations will be used in Sec. V to evaluate the integrals in Eqs. (10) and (11).

The orbit expressions derived in this section are valid for an arbitrary density profile $n_0(x)$ of a single component plasma producing a self-electric field $E_0(x)\hat{x}$ with $dE_0/dx = 4\pi q n_0$. The requirement that the plasma be in Vlasov equilibrium provides another relation between n_0 and E_0

through the distribution function. The problem of determining n_0 and E_0 self-consistently is treated in the next section.

IV. VLASOV EQUILIBRIUM

In this section a Vlasov equilibrium distribution function describing a single component plasma slab (of finite width in x) immersed in a strong uniform external magnetic field $B_0\hat{z}$ (see Fig. 1) is constructed and density profiles consistent with the self-electric fields are obtained. The equilibrium is, however, not a thermal equilibrium and hence the phenomena to be studied using this distribution function must occur on a time scale short compared to the characteristic time of plasma expansion produced by interparticle collisions.

In constructing the distribution function $f_0(x,\mathbf{v})$, motion along the z direction is ignored as in the previous sections and thus $\mathbf{v}$ refers to the velocity in the xy plane. Any distribution function constructed from the single particle constants of the motion, energy $\epsilon = \frac{1}{2}mv^2 + q\phi_0(x)$, and the canonical momentum $p_y = m(v_y + \Omega x)$ represents a Vlasov equilibrium distribution. The specific choice

$$f_0 = C\exp\{-[v^2 + (2q/m)\phi_0(x)]/2\bar{v}^2 - (x + v_y/\Omega)^2/2l^2\}, \tag{36}$$

where $\bar{v}$ and l are given parameters, C a normalization constant, and $\phi_0(x)$ the self-consistent electric potential, describes a realistic bell-shaped density profile peaked at $x = 0$. With a rearrangement of terms, f_0 can be put in the form

$$f_0(x,\mathbf{v}) = C\exp\left[-\frac{v_x^2}{2\bar{v}^2} - \frac{l^2 + r_c^2}{2l^2\bar{v}^2}\left(v_y + x\Omega\frac{r_c^2}{l^2 + r_c^2}\right)^2 - \frac{x^2}{2(l^2 + r_c^2)} - \frac{q\phi_0(x)}{m\bar{v}^2}\right], \tag{37}$$

where $r_c = \bar{v}/\Omega$, showing clearly that in a local frame drifting with velocity

$$\mathbf{v}_d = -x\Omega[r_c^2/(l^2 + r_c^2)]\hat{y}, \tag{38}$$

the distribution function $f_0(x,\mathbf{v})$ is a bi-Maxwellian with the effective temperatures in the x and y directions being

$$T_x = m\bar{v}^2, \tag{39a}$$

$$T_y = ml^2\bar{v}^2/(l^2 + r_c^2). \tag{39b}$$

The potential $\phi_0(x)$ in Eqs. (36) and (37) is not arbitrary but has to be determined as the self-consistent solution to Poisson's equation

$$\frac{d^2\phi_0}{dx^2} = -4\pi q n_0(x) = -4\pi q n_0(0)\exp\left(-\frac{q}{m\bar{v}^2}[\phi_0(x) - \phi_0(0)] - \frac{x^2}{2(l^2 + r_c^2)}\right), \tag{40}$$

where $n_0(x)$ is obtained by integrating $f_0(x,\mathbf{v})$ over velocity. Using this expression for $n_0(x)$ in terms of $\phi_0(x)$, it can be shown that the drift velocity $\mathbf{v}_D$ given by Eq. (38) is the sum of the drift velocity $v_E(x)\hat{y} = -c(\nabla\phi_0\times\hat{z})/B_0$ resulting from the equilibrium electric field and the diamagnetic drift velocity $-\bar{v}^2(\nabla n_0\times\hat{z})/\Omega n_0$.

The solution of the nonlinear differential equation (40) for the self-consistent potential $\phi_0(x)$ is facilitated by the introduction of the scaled variables

$$\psi = -(2/m\bar{v}^2)[\phi_0(x) - \phi_0(0)] - x^2/2(l^2 + r_c^2), \tag{41a}$$

$$\lambda_D^2 = m\bar{v}^2/4\pi q n_0(0), \tag{41b}$$

$$\xi = x/\lambda_D, \tag{41c}$$

$$A = \lambda_D^2/(l^2 + r_c^2), \tag{41d}$$

in terms of which Eq. (40) takes the form

$$\frac{d^2\psi}{d\xi^2} = e^{\psi} - A. \tag{42}$$

Since $n_0(\xi) = n_0(0)\exp\psi$, ψ must approach $-\infty$ for $|\xi| \to \infty$ in order that the plasma be bounded. From the structure of Eq. (42), it follows that the necessary and sufficient condition for a bounded density profile is $A > 1$, which from Eq. (41d) implies $\lambda_D > r_c$ or $\Omega > \omega_p(0)$ (for all values of $\bar{v}$). The last inequality is the slab analog of the Brillouin condition setting the limit for the maximum density that can be confined by a given magnetic field. Since the calculation of the unperturbed orbits (Sec. III) is possible only when r_c is small compared to the scale length of variation of the equilibrium density profile, the present study assumed $\Omega \gg \omega_p(0)$.

The physical significance of the parameter A can be understood by noting that a particle drifting with velocity $\mathbf{v}_D$ across the magnetic field $B_0\hat{z}$ experiences in its rest frame an effective electric field $\mathbf{v}_D\times B_0\hat{z}/c$. This field can be equivalently thought of as arising from a fictitious neutralizing background consisting of charges $-q$ having the density [using Eqs. (38) and (41d)]

$$N = -(1/4\pi q)\nabla\cdot[(\mathbf{v}_D\times B_0\hat{z})/c] = An_0(0). \tag{43}$$

Thus the confining effect of the magnetic field can be simulated by a stationary uniform charge-density neutralizing background. If $A > 1$, then $N > n_0(0)$ and the confining force caused by N overcomes the self-repulsion of the plasma. On the other hand, if $A < 1$, then $N < n_0(0)$ and the plasma is unconfined. If $A = 1$, the two forces are in equilibrium for $n_0(x) = n_0(0) = N$.

The self-consistent density profiles and the corresponding electric field potentials obtained from numerical solutions of Eq. (42) are displayed in Fig. 2 for the cases $A = 1.1$ and $A = 2$. The closer the value of A is to 1, the wider the density profile is (as measured in terms of the central Debye length λ_D). Also, in the limit $A \to 1$, the width of the density falloff region measured in terms of λ_D approaches a constant ~ 5. Note that from Eq. (41d), the assumption $r_c \ll \lambda_D$ implies $l \simeq \lambda_D$ for values of A close to unity.

As indicated at the beginning of this section, the distribution function f_0 given by Eq. (36) describes a Vlasov equilibrium and not a thermal equilibrium. The distribution function $\exp(\alpha\epsilon + \beta p_y)$ (α and β being constants) associated with thermal equilibrium, however, does not describe a bounded plasma slab; the corresponding self-consistent density profile increases monotonically on either side of $x = 0$. The nonthermal equilibrium nature of f_0 given by Eq. (36) is reflected in the fact that the total drift [Eq. (38)] has a

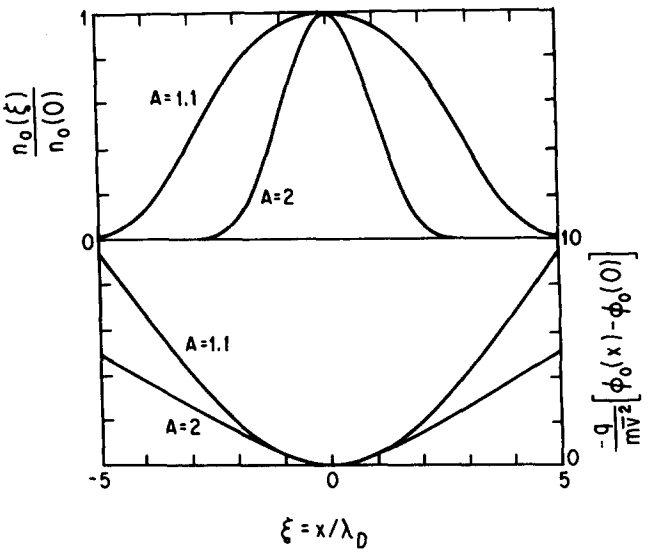

FIG. 2. Self-consistent density profiles (top) and corresponding electric potentials (bottom) in a single component plasma for $A = 1.1$, 2.0 [Eq. (42)].

shear. Inclusion of collisions would create a collisional drag force (acting along $\hat{y}$) between neighboring layers moving relative to each other. This force, in the presence of the magnetic field $B_0\hat{z}$, creates a new drift along $\hat{x}$ as a result of which the plasma expands. Thus collisions will destroy the Vlasov equilibrium described by f_0. The wave analysis is therefore applicable only to time scales short compared to the collisional expansion time.

V. COLD PLASMA RESPONSE

The cold plasma response is derived in this section as a benchmark and attention is focused on its singularities (which are rectified when thermal effects are included). For this purpose, it is convenient to truncate the differential equation for ϕ_1 obtained in Sec. II to include only the lowest-order thermal effects. Using Eqs. (30)–(35), and the equilibrium Vlasov equation,

$$v_x \frac{\partial f_0}{\partial x} + \Omega u_y \frac{\partial f_0}{\partial v_x} - \Omega v_x \frac{\partial f_0}{\partial v_y} = 0, \tag{44}$$

the truncated version of Eq. (11) can be put in the self-adjoint form,

$$\frac{d^2\phi_1}{dx^2} - k_y^2\phi_1 = -\frac{4\pi q^2}{m}\left\{\left(\beta_0 + \beta_1' + \frac{1}{2}\beta_2'' + \frac{1}{6}\beta_3'''\right)\phi_1 + \frac{d}{dx}\left[\left(\alpha_1 + \frac{1}{2}\beta_2 + \frac{1}{6}\beta_3'\right)\frac{d\phi_1}{dx}\right] + \frac{d^2}{dx^2}\left(\frac{1}{6}\alpha_3\frac{d^2\phi_1}{dx^2}\right)\right\}. \tag{45}$$

In Eq. (45), primes denote derivatives with respect to x and

$$\alpha_p = \left\langle \frac{\partial f_0}{\partial v_x} \right\rangle_p, \tag{46}$$

$$\beta_p = ik_y \left\langle \frac{\partial f_0}{\partial v_y} \right\rangle_p, \tag{47}$$

where the operator $\langle\ \rangle_p$ is defined by

$$\langle g(x,\mathbf{v})\rangle_p = \int d\mathbf{v}\, g \int_{-\infty}^{0} d\tau\, e^{-i\omega\tau}[x - X(-\tau,x,\mathbf{v})]^p \times \exp[-ik_y \tilde{Y}(-\tau,x,\mathbf{v})], \tag{48}$$

with X and $\tilde{Y}$ given by Eqs. (30)–(33).

Equation (45) includes all the lowest-order thermal corrections (proportional to $\bar{v}^2$). Its self-adjoint structure is a reflection of the conservation of energy in this system.

Ignoring the thermal corrections to Eq. (45) gives the cold plasma response. In the cold limit, the only contributions to the right-hand side of Eq. (45) are

$$\beta_0 \simeq -k_y \int d\mathbf{v} \frac{\partial f_0}{\partial v_y}\left[\frac{1}{\omega_1} + \frac{k_y\Omega^2 u_y}{2\Omega_1^3}\left(\frac{1}{\omega_1 - \nu} - \frac{1}{\omega_1 + \nu}\right)\right] \rightarrow k_y \frac{\Omega n_0}{\Omega_1^2}\frac{\partial}{\partial x}\left(\frac{1}{\omega_D}\right) + \frac{k_y^2\Omega^2}{\Omega_1^2}\frac{n_0}{\omega_D^2 - \Omega_1^2}, \tag{49a}$$

$$\beta_1 \simeq k_y \frac{\Omega}{\Omega_1^2}\int d\mathbf{v} \frac{\partial f_0}{\partial v_y} u_y\left(\frac{1}{\omega_1} - \frac{\frac{1}{2}}{\omega_1 - \nu} - \frac{\frac{1}{2}}{\omega_1 + \nu}\right) \rightarrow \frac{k_y\Omega}{\omega_D}\frac{n_0}{\omega_D^2 - \Omega_1^2}, \tag{49b}$$

and

$$\alpha_1 \simeq -\frac{1}{2\Omega_1}\int d\mathbf{v} f_0\left(\frac{1}{\omega_1 - \nu} - \frac{1}{\omega_1 + \nu}\right) \rightarrow -\frac{n_0}{\omega_D^2 - \Omega_1^2}, \tag{49c}$$

where partial integrations with respect to v_y and the normalization condition $\int d\mathbf{v} f_0 = n_0(x)$ have been used; the quantity ω_1 is defined by Eq. (12) and ω_D is defined as

$$\omega_D = \omega + (k_y/\Omega)(q/m)E_0(x) = \omega - k_y v_E(x). \tag{50}$$

Equations (45) and (49) yield the second-order differential equation for the cold plasma response

$$\frac{d}{dx}\left[\left(1 - \frac{\omega_p^2}{\omega_D^2 - \Omega_1^2}\right)\frac{d\phi_1}{dx}\right] - \left[\frac{k_y\Omega}{\omega_D}\frac{d}{dx}\left(1 - \frac{\omega_p^2}{\omega_D^2 - \Omega_1^2}\right) + k_y^2\left(\frac{\omega_p^2}{\omega_D^2 - \Omega_1^2}\right)\right]\phi_1 = 0. \tag{51}$$

It should be noted that in the limit of zero temperature, the distribution function f_0 of Sec. IV leads to a rectangular density profile, since the width of the density falloff region in terms of the central Debye length λ_D is a constant. [For a nonzero density profile one must also have $A \rightarrow 1$, where A is defined by Eq. (41d).] Thus $E_0(x)$ and $v_E(x)$ are linear functions of x and ω_p^2 and Ω_1^2 are position independent within the plasma. The result (51) is, however, more general [since the steps used, Eqs. (49), in deriving it do not depend on any specific choice of f_0] and is valid for any density profile that can be self-consistently obtained from an f_0 in the cold limit.

As indicated in the Introduction, Eq. (51) can be obtained from the neutral plasma result by including the Doppler shift resulting from $\mathbf{E}\times\mathbf{B}$ drift and by replacing the cyclotron frequency Ω by the effective single particle gyration frequency $\Omega_1 = (\Omega^2 - \omega_p^2)^{1/2}$. The replacement $\Omega \rightarrow \Omega_1$

should not, however, be confused with the transformation $\Omega \to \Omega - 2\omega_e$ used by Davidson[8] to formally obtain non-neutral plasma waves (for a rigid rotor of angular frequency ω_e) from neutral plasma results. The physical origins of the two transformations are entirely different. The latter is caused by the Coriolis force in the rotating frame whereas the former is caused by the modification of the particle orbit resulting from the gradient in the electric field. In fact, $\Omega_1(r)$ for the general cylindrical case has the form

$$\Omega_1(r) = \left[[\Omega - 2\omega_e(r)] \left(\Omega - 2\omega_e(r) - r \frac{d\omega_e}{dr}(r) \right) \right]^{1/2}, \tag{52}$$

where

$$\omega_e(r) = \frac{1}{\Omega r^2} \int_0^r dr'\, r' \omega_p^2(r') \tag{53}$$

is the $\mathbf{E} \times \mathbf{B}$ rotation frequency. For a rigid rotor, ω_p^2 and ω_e are constant and $\Omega_1 \to \Omega - 2\omega_e$. However, the modification discussed in the present paper is associated with the $d\omega_e/dr$ term and can be obtained in the transition to the slab model by considering a cylindrical shell $R < r < R + \Delta$ and taking the limit $R \gg \Delta$. Then $\omega_e \sim \omega_p^2 \Delta/\Omega R \to 0$, $r\, d\omega_e/dr \to \omega_p^2/\Omega$, and $\Omega_1(r) \to [\Omega^2 - \omega_p^2(r)]^{1/2}$.

Solutions of Eq. (51) are next investigated for the cases $k_y = 0$ and $k_y \neq 0$.

(a) $k_y = 0$: In this case Eq. (51) can be integrated once with respect to x to yield

$$[1 - \omega_p^2/(\omega^2 - \Omega_1^2)] E_{1x} = E_c$$

or

$$E_{1x} = \frac{\omega^2 - \Omega_1^2}{\omega^2 - \Omega^2} E_c = \left(1 + \frac{\omega_p^2(x)}{\omega^2 - \Omega^2} \right) E_c, \tag{54}$$

where E_c is the vacuum field generated by external capacitor plates assumed to be located where the plasma density is negligible. Equation (54) predicts that E_1 has a global resonance when $\omega = \Omega$ and has local nulls at layers where $\omega = \Omega_1(x)$. It is shown later that thermal effects modify both these features and introduce energy absorption by particles at the $\omega = \Omega_1(x)$ layers. As follows from Eq. (54), a plot of E_{1x} vs x (for $E_c > 0$, $\omega < \Omega$) is identical to the plot of ω_p^2 vs x (Fig. 2), inverted and repositioned vertically so as to pass through zero at the $\omega = \Omega_1(x)$ layers.

(b) $k_y \neq 0$: Solutions of Eq. (51) for $k_y \neq 0$ describe waves propagating along the y direction. Equation (51) has singularities at layers where $\omega_D \equiv \omega - k_y v_E(x) = \pm \Omega_1(x)$, $\omega_D = (\Omega_1^2 + \omega_p^2)^{1/2} = \pm \Omega$, and $\omega_D = 0$; a study of the behavior near these layers shows that the exact solutions of the equation are finite and continuous at the $\omega_D = \pm \Omega_1(x)$ layers while at the $\omega_D = \pm \Omega$ layers (and also at the $\omega_D = 0$ layer), one of the two linearly independent solutions exhibits a logarithmic singularity. These singularities are, however, removed when thermal effects are included, as shown in the next section. A detailed analysis of the properties of Eq. (51) is outside the scope of the present publication.

From Gauss' law, the electric field $E_0(x)$ [and hence $v_E(x) = qE_0(x)/(m\Omega)$] increases monotonically with x, passing through zero at $x = 0$. Thus $\omega_D = \omega - k_y v_E(x)$ is a monotonic function of x and the singularity $\omega_D = \Omega$ can occur, at most, at one value of x. Similarly, one can have at most one $\omega_D = 0$ singularity layer inside the plasma. On the other hand, since $\Omega_1(x)$ is an even function of x having a single minimum at $x = 0$, the equation $\omega_D = \Omega_1(x)$ can have 0, 1, or 2 roots depending on the values of ω and k_y. Figure 3 displays the solution of Eq. (51) for the density profile shown in dashed lines and for $\omega_p^{(0)}/\Omega = 0.1$, $\omega/\Omega = 0.994$, and $k_y x_b = 0.04$; the boundary conditions are $\phi_1(-x_b) \neq 0$, $\phi_1(x_b) = 0$. The value of ω and k_y are such that the singularities $\omega_D = \Omega$ and $\omega_D = 0$ are absent. The equation $\omega_D = \Omega_1(x)$ has two solutions indicated in the figure, but at these layers, the solution and its derivative are continuous.

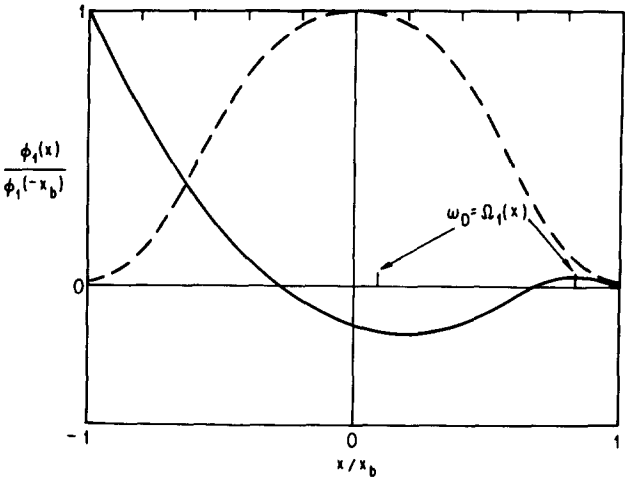

FIG. 3. The solution of Eq. (51) for the density profile shown in dashed lines and for $\omega_p(0)/\Omega = 0.1$, $\omega/\Omega = 0.9975$, $k_y x_b = 0.04$. The boundary conditions are $\phi_1(-x_b) \neq 0$, $\phi_1(x_b) = 0$.

VI. THERMAL EFFECTS

Two nonzero-temperature effects are considered here. The first one, a kr_c effect, gives rise to successively higher-order thermal modes (analogs of neutral plasma Bernstein modes) as higher-order terms in powers of kr_c are included in the differential equation for ϕ_1. Equation (45), which is accurate to $O(k^2 r_c^2)$, describes the behavior of waves near the first two harmonics of the gyrofrequency Ω_1 (and also the low frequency diocotron wave). The second effect arises for nonzero values of r_c/L because the equilibrium electric field $E_0(x)\hat{x}$ modifies the single particle orbit and in particular introduces a velocity dependence in the particle gyration frequency. This effect causes the absorption of wave energy by particles at layers where $\omega - k_y v_E(x) = \pm \Omega_1(x)$ and $\omega - k_y v_E(x) = 0$. For clarity of exposition, each of these effects is considered separately. Thus approximate equilibrium particle orbits,

$$x - X(-\tau, x, \mathbf{v}) = (v_x/\Omega_1)\sin \Omega_1 \tau + (\Omega u_y/\Omega_1^2)(\cos \Omega_1 \tau - 1), \tag{55a}$$

$$\tilde{Y}(-\tau, x, \mathbf{v}) = -v_E(x)\tau + (\Omega v_x/\Omega_1^2)(\cos \Omega_1 \tau - 1) - (\Omega^2 u_y/\Omega_1^2)\sin \Omega_1 \tau, \tag{55b}$$

$$\Omega_1(x) = [\Omega^2 - \omega_p^2(x)]^{1/2}, \tag{55c}$$

$$u_y = v_y + (1/\Omega)(q/m)E_0(x) = v_y - v_E(x), \tag{55d}$$

which do not include correction resulting from nonzero r_c/L [see Eqs. (30)–(34)], are used to evaluate the right-hand side of Eq. (45) to illustrate the lowest-order kr_c effect. To highlight the r_c/L effect, equilibrium particle orbits with the most important nonzero r_c/L corrections [i.e., Eqs. (55) with the replacements $\Omega_1(x)\tau \to \nu(x,v)\tau$ and $v_E(x)\tau \to v_d(x,v)\tau$, where ν and v_d are given by Eqs. (31) and (34), respectively] are used in the differential equation for ϕ_1 that contains no finite kr_c corrections; the result corresponds to the modification of the "cold" wave equation (51) when the integrals β_0, β_1, and α_0 [Eqs. (49)] are evaluated using the expressions (31) and (34) for ν and v_d, respectively.

As in the previous section, the cases $k_y = 0$ and $k_y \neq 0$ are considered separately.

(a) $k_y = 0$

(i) kr_c effects: For $k_y = 0$, it follows from Eq. (47) that $\beta_p = 0$ for all p. Thus there is no term proportional to ϕ_1 in Eq. (45), which can now be integrated once with respect to x to yield a second-order differential equation for the wave electric field $E_{1x} = -d\phi_1/dx$:

$$\left(1 + \frac{4\pi q^2}{m}\alpha_1(k_y = 0)\right)E_{1x} + \frac{1}{6}\frac{d}{dx}\left(\frac{4\pi q^2}{m}\alpha_3(k_y = 0)\frac{dE_1}{dx}\right) = E_c, \tag{56}$$

where α_1 and α_3 are given by Eqs. (46) and (48) with $k_y = 0$. Using $(x - X)$ from Eq. (55), the time integral in Eq. (48) can be readily done and the result [using Eq. (44)] expressed in terms of integrals of the form $\int dv\, u_y^m v_x^n f_0$. Such integrals can be reduced to powers of $\bar{v}$ multiplied by the density $n_0(x)$ (or its derivatives) as shown in the Appendix. Using these results, one obtains

$$(4\pi q^2/m)\alpha_1(k_y = 0) = -\omega_p^2/(\omega^2 - \Omega_1^2) \tag{57a}$$

and

$$\frac{4\pi q^2}{m}\alpha_3(k_y = 0) = -6\bar{v}^2\frac{\omega_p^2}{\Omega_1^2}\left(\frac{1}{\omega^2 - \Omega_1^2} - \frac{1}{\omega^2 - 4\Omega_1^2}\right). \tag{57b}$$

Thus Eq. (56) takes the form

$$-\frac{d}{dx}\left[r_c^2\frac{\Omega^2}{\Omega_1^2}\left(\frac{1}{\omega^2 - \Omega_1^2} - \frac{1}{\omega^2 - 4\Omega_1^2}\right)\frac{dE_1}{dx}\right] + \left(1 - \frac{\omega_p^2}{\omega^2 - \Omega_1^2}\right)E_{1x} = E_c, \tag{58}$$

where the first term on the left-hand side is the lowest-order (quadratic) kr_c correction to the cold plasma result, Eq. (54).

Replacing dE_1/dx by ik_xE_1 in Eq. (58) with the driver $E_c = 0$ yields the approximate WKB dispersion relation

$$k_x = iQ \pm \left(-Q^2 + \frac{(\omega^2 - \Omega^2)(\omega^2 - 4\Omega_1^2)}{3r_c^2\omega_p^2\Omega^2}\right)^{1/2}, \tag{59}$$

where

$$Q = \frac{1}{2}\frac{d\omega_p^2/dx}{\omega_p^2}\frac{(\omega^2 - \Omega^2)(\omega^2 - 4\Omega^2) - 4\omega_p^4}{(\omega^2 - \Omega_1^2)(\omega^2 - 4\Omega_1^2)}. \tag{60}$$

The WKB wavenumber k_x given by Eq. (59) has singularities at $\omega = \Omega_1(x)$ and $\omega = 2\Omega_1(x)$. An analysis of the differential equation (58) near these layers, however, shows that the two linearly independent solutions of the homogeneous differential equation are both finite and continuous at these layers.

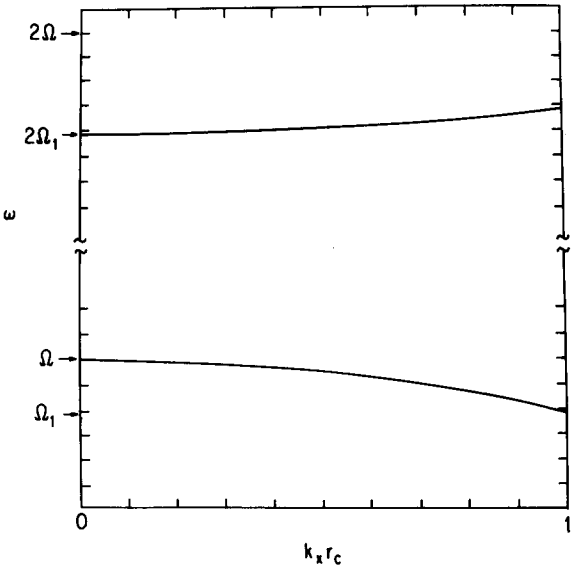

FIG. 4. Warm plasma dispersion obtained from the approximate WKB solution, Eq. (61). These non-neutral Bernstein modes have cutoffs at the "upper hybrid frequency" Ω and the second harmonic of the single particle gyrofrequency $\Omega_1(x)$.

Ignoring the density derivative correction caused by Q, Eq. (59) takes the form of a Bernstein wave dispersion relation (near cutoff)

$$(k_x r_c)^2 = (\omega^2 - \Omega^2)[\omega^2 - 4\Omega_1^2(x)]/3\Omega^2\omega_p^2(x), \tag{61}$$

which is displayed in Fig. 4. These non-neutral Bernstein modes propagate for $\omega < \Omega$, $\omega > 2\Omega_1$ [with cutoffs at $\omega = \Omega$, $2\Omega_1$], which is consistent with the neutral plasma results since in the present single component plasma, the single particle gyrofrequency is Ω_1 and the collective "upper hybrid" frequency is $\Omega = (\Omega_1^2 + \omega_p^2)^{1/2}$. Note that the condition $k_x r_c < 1$ required for the validity of Eq. (58) implies, from Eq. (61), that the frequency ω be close to the cutoff values Ω, $2\Omega_1$.

As mentioned earlier in Sec. V(a), the presence of thermal modes for nonzero values of kr_c removes the global resonance of the cold plasma E_{1x} at $\omega = \Omega$. For capacitor plate antennae positioned at $x = \pm x_b$, Eq. (58) can be integrated twice for $\omega = \Omega$ to yield

$$E_{1x}(x) \simeq E_c[1 - (x^2 - x_b^2)/2r_c^2], \tag{62a}$$

so that

$$E_{1x}(0) \simeq E_c x_b^2/2r_c^2 \tag{62b}$$

is large but finite.

The wave electric field E_{1x} produced by a uniform external field E_c can be obtained for any ω by numerically integrating Eq. (58). The undriven ($E_c = 0$) waveforms have a definite parity (in x) as is clear from Eq. (58). The even solution, satisfying the conditions $E_{1x}(0) = 1$ and

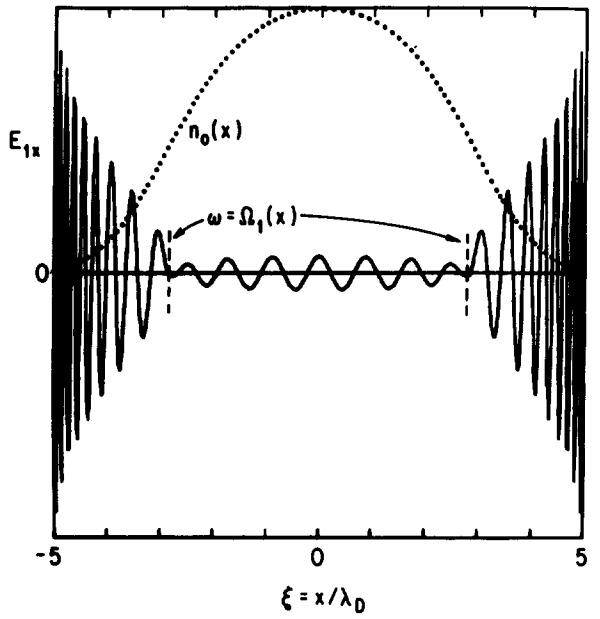

FIG. 5. The undriven solution E_{1x} (of even parity) of Eq. (58) for the $A = 1.1$ density profile of Fig. 2 and for $\omega_p(0)/\Omega \equiv r_c/\lambda_D = 0.1$. The boundary conditions are $E_{1x}(0) \neq 0$ and $E'_{1x}(0) = 0$. The scale for E_{1x} is arbitrary.

$dE_{1x}/dx|_{x=0} = 0$ is shown in Fig. 5 for the $A = 1.1$ equilibrium density profile with $\omega_p(0)/\Omega = r_c/\lambda_D = 0.1$ and $\omega/\Omega = 0.9975$.

The increase in the wave amplitude near the plasma edge seen in Fig. 5 does not result from any resonance but is related to the decreasing density profile. This can be readily seen from the approximate WKB solutions (59) and (60). Near the ends, $\omega_p^2 \to 0$ and hence $Q \simeq (d/dx)(\ln \omega_p)$ and the WKB wave amplitude $\sim \exp(-\int dx \operatorname{Im} k_x) \sim \omega_p^{-1}$ and thus is proportional to $[n_0(x)]^{-1/2}$.

When the driver is on ($E_c \neq 0$), the thermal mode pattern appears superposed on the cold plasma response given by Eq. (54). Figure 6 displays E_{1x} for the driven case for the same parameter values $A = 1.1$, $\omega_p(0)/\Omega = 0.1$, $\omega/\Omega = 0.9975$, and the boundary conditions $E_{1x} = E_c$ at $x = \pm x_b$, the position of the capacitor plates. The collective electric field in the plasma becomes large as the driver frequency ω approaches values ω_n for which the undriven E_{1x} has nodes at $x = \pm x_b$. These are the analogs of Tonks–Dattner resonances[9] in neutral plasmas. Quantizing $k_x(x,\omega)$ given by Eq. (61) to fit the antenna spacing yields approximate values of ω_n. For $\omega < \Omega$, $k_x(x,\omega)$ is real for all x and the quantization condition determining ω_n takes the form

$$\int_{-x_b}^{x_b} dx\, k_x(x,\omega_n) \simeq \frac{n\pi}{2x_b}. \tag{63}$$

The undriven solutions have even parity (in x) if n is an odd integer and have odd parity if n is even. The solutions displayed in Figs. 5 and 6 correspond to $n = 47$ for which ω_n has the value $0.997\,508\,65\Omega$. The amplitude of the thermal mode defined as the difference in values of the central extremum and the neighboring extremum of Fig. 6, is shown as a function of ω in Fig. 7.

Near the second harmonic, Eq. (61) predicts propagation if $\omega > 2\Omega_1(x)$. Since $\Omega_1(x)$ has a minimum at $x = 0$, a capacitor plate antenna oscillating at a frequency ω such that $2\Omega_1(0) < \omega < 2\Omega$ creates a thermal mode pattern [superposed on the almost constant cold plasma response given by Eq. (54)] which has a propagating character in the center of the plasma slab and is evanescent near the edges. Again, the amplitude of the thermal mode pattern is large for certain discrete values of ω. Figure 8 displays the numerical solution for E_{1x} when $A = 1.1$, $\omega_p(0)/\Omega \equiv r_c/\lambda_D = 0.1$, $\omega/\Omega = 1.996$ with $E_{1x}(\pm x_b) = E_c$.

(ii) r_c/L effect: For $k_y = 0$, the coefficients β_0 and β_1 are zero, and Eqs. (49c), (31), and (37) yield

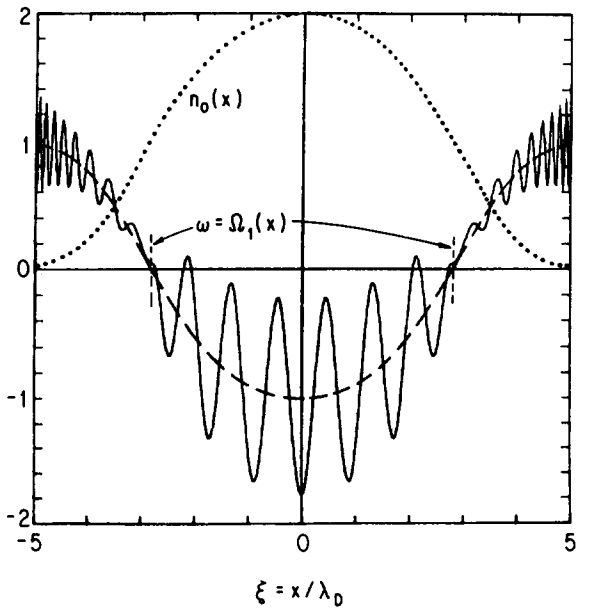

FIG. 6. The driven solution E_{1x} of Eq. (58) for the $A = 1.1$ density profile of Fig. 2 and for $\omega_p(0)/\Omega \equiv r_c/\lambda_D = 0.1$ and $\omega/\Omega = 0.9975$. Here $E_{1x}(-x_b) = E_{1x}(x_b) = E_c$. The cold plasma response is shown by the dashed line.

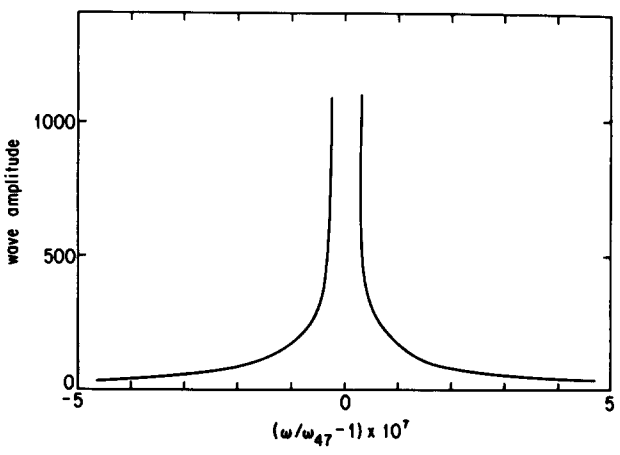

FIG. 7. The amplitude of the thermal pattern (defined as the difference between the central minimum and the neighboring maximum in the driven solution E_{1x}/E_c of Fig. 6) as a function of ω near $\omega_n = 0.997\,508\,65\Omega$ corresponding to $n = 47$ [see Eq. (63)].

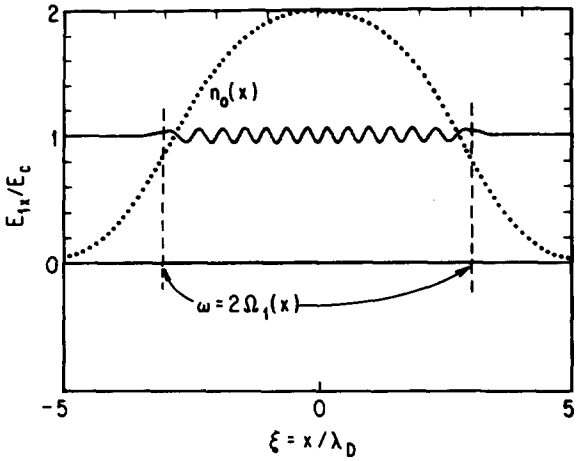

FIG. 8. The driven solution E_{1x} of Eq. (58) near the second harmonic. Here $A = 1.1$, $\omega_p(0)/\Omega = 0.1$, $\omega/\Omega = 1.996$, and $E_{1x}(-x_b) = E_{1x}(x_b) = E_c$.

$$\alpha_1 \simeq -\frac{n_0(x)}{2\Omega_1}\left(\frac{m}{2\pi T_y}\right)^{1/2}\int_{-\infty}^{\infty} dv_y\, e^{-m(v_y-v_D)^2/2T_y} \times\left[\left(\omega-\Omega_1+\frac{1}{2\Omega^2}\frac{d\omega_p^2}{dx}(v_y-v_D)\right)^{-1} -\left(\omega+\Omega_1-\frac{1}{2\Omega^2}\frac{d\omega_p^2}{dx}(v_y-v_D)\right)^{-1}\right] = \frac{n_0}{2\Omega_1\Delta\omega}\left[Z\left(\frac{\omega-\Omega_1}{\Delta\omega}\right)-Z\left(\frac{\omega+\Omega_1}{\Delta\omega}\right)\right], \quad (64)$$

where Z is the plasma dispersion function[10] and

$$\Delta\omega = \frac{1}{\Omega^2}\left|\frac{d\omega_p^2}{dx}\right|\left(\frac{T_y}{2m}\right)^{1/2} = r_c l\left|\frac{d\omega_p^2}{dx}\right|\left[2\Omega^2(r_c^2+l^2)\right]^{-1/2} \simeq O\left(\frac{r_c}{L}\right)\left(\frac{\omega_p^2}{\Omega^2}\right)\Omega. \quad (65)$$

In obtaining Eq. (64), the usual adiabatic switching approximation (i.e., $\omega = \omega + i0$) is made. Using Eq. (64), the cold plasma response (54) is modified (for $\omega > 0$) into

$$\left\{1+\frac{\omega_p^2}{2\Omega_1}\left[\frac{1}{\Delta\omega}Z\left(\frac{\omega-\Omega_1}{\Delta\omega}\right)+\frac{1}{\omega+\Omega_1}\right]\right\}E_{1x} = E_c \quad (66)$$

by the inclusion of nonzero r_c/L corrections to the equilibrium single particle orbits. At layers $\omega = \Omega_1(x)$, where the cold plasma E_{1x} vanishes, the Z function is finite (and has the value $i\pi^{1/2}$) and E_{1x} is no longer zero ($\mathrm{Im}\, E_{1x} \sim O[(r_c/L)E_c]$, $\mathrm{Re}\, E_{1x} \sim O[(r_c/L)^2 E_c]$). Figure 9 displays the real and imaginary parts of E_{1x} produced by an external driver E_c for the parameter values $A = 1.1$, $\omega_p(0)/\Omega = 0.1$, and $\omega/\Omega = 0.9975$.

The complex character of the Z functions also implies that it is possible for the particles at the resonant layers to absorb energy from the fields. The rate of energy absorption per unit volume is $1/4(j_{1x}^* E_{1x} + j_{1x} E_{1x}^*)$, where the linearized plasma current is $j_{1x} = i\omega(E_c - E_{1x})/4\pi$. Using Eq. (66), the power absorbed per unit volume is

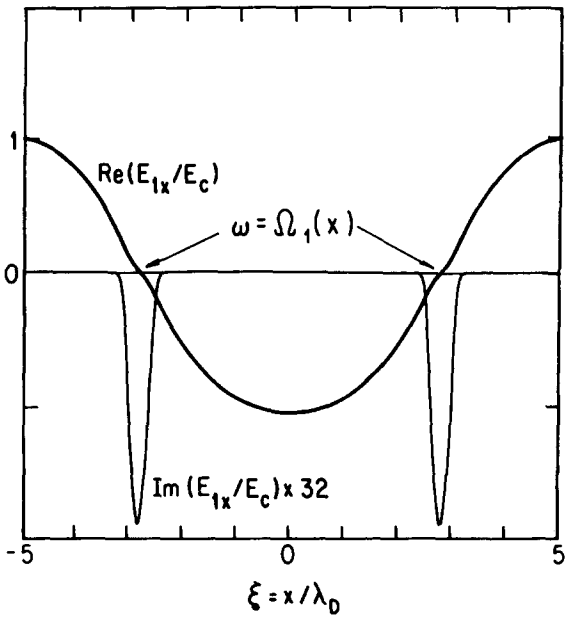

FIG. 9. Real and imaginary parts of the electric field E_{1x} given by Eq. (66) for $A = 1.1$, $\omega_p(0)/\Omega = 0.1$, and $\omega/\Omega = 0.9975$.

$$P = -\frac{\omega}{8\pi}E_c^2\frac{\mathrm{Im}\, E_{1x}}{E_c} = \frac{\omega}{8\pi}E_c^2\frac{\omega_p^2}{2\Omega_1^2}\frac{1}{\Delta\omega}\mathrm{Im}\, Z\left(\frac{\omega-\Omega_1}{\Delta\omega}\right) \times\left\{\left|1+\frac{\omega_p^2}{2\Omega_1}\left[\frac{1}{\Delta\omega}Z\left(\frac{\omega-\Omega_1}{\Delta\omega}\right)+\frac{1}{\omega+\Omega_1}\right]\right|^2\right\}^{-1}. \quad (67)$$

The normalized power absorption $8\pi P/\omega E_c^2$ is just the negative of $\mathrm{Im}(E_{1x}/E_c)$ displayed in Fig. 9. The width of the resonance region where the energy absorption takes place is $O(r_c)$.

The physical mechanism for energy absorption is similar to the familiar cyclotron damping (even though in the present case $k_z = 0$). Particles in the resonant region experience a collective electric field which continuously accelerates them or decelerates them depending on their phase with respect to the field. Since the rate of change of energy is $q\mathbf{E}_1 \cdot \mathbf{v}$, where $\mathbf{v}$ is the particle velocity, the accelerating particles gain energy at a faster rate than the decelerating particles lose it. Thus the energy transfer is always unidirectional—from the wave to the particles. The largest number of particles whose velocity-dependent oscillation frequency ν [Eq. (31)] can match the wave frequency are at the layer where $\omega = \Omega_1(x)$ and their number falls off rapidly on either side of this layer within roughly a Larmor radius. Thus the energy absorption profile is a bell-shaped curve of width $\sim O(r_c)$ centered at the $\omega = \Omega_1(x)$ layer.

Allowing nonzero k_z in the present problem produces conventional cyclotron damping. This additional damping is negligible compared to the finite r_c/L damping if

$$k_z(T_z/m)^{1/2} \ll \Delta\omega$$

or

$$k_z^{-1} \gg L(\Omega/\omega_p)^2(T_x/T_z)^{1/2}. \quad (68)$$

(b) $k_y \neq 0$

(i) kr_c effect: Evaluation of the coefficients α_m and β_m in Eq. (45) using the orbit expressions (55) leads to a fourth-order differential equation for ϕ_1, which includes the lowest-order (quadratic) finite kr_c corrections to the cold plasma terms. The general differential equation that includes the density gradient effects and the drift effects on the non-neutral Bernstein modes (and also the low frequency diocotron mode) has been obtained but since it is rather lengthy, is not presented here. An extension of the approximate dispersion (61) to include nonzero k_y can be readily obtained by replacing d/dx by ik_x in Eq. (45) and ignoring the primed quantities. This leads to

$$k_x^2 + k_y^2 = (4\pi q^2/m)\left[\beta_0 - k_x^2(\alpha_1 + \tfrac{1}{2}\beta_2) + \tfrac{1}{6}k_x^4\alpha_3\right]. \tag{69}$$

Using Eq. (55) and ignoring derivatives with respect to x,

$$\beta_0 \simeq \frac{k_y^2\Omega^2}{\Omega_1^2}\frac{n_0}{\omega_D^2-\Omega_1^2} + \frac{3k_y^4\Omega^4}{\Omega_1^4}\frac{\bar{v}^2 n_0}{(\omega_D^2-\Omega_1^2)(\omega_D^2-4\Omega_1^2)}, \tag{70a}$$

$$\beta_2 = -\frac{6k_y^2\Omega^2\bar{v}^2}{\Omega_1^2}\frac{n_0}{(\omega_D^2-\Omega_1^2)(\omega_D^2-4\Omega_1^2)}, \tag{70b}$$

$$\alpha_1 = -\frac{n_0}{\omega_D^2-\Omega_1^2} - \frac{3k_y^2\Omega^2\bar{v}^2}{\Omega_1^2}\frac{n_0}{(\omega_D^2-\Omega_1^2)(\omega_D^2-4\Omega_1^2)}, \tag{70c}$$

$$\alpha_3 = 18\bar{v}^2\frac{n_0}{(\omega_D^2-\Omega_1^2)(\omega_D^2-4\Omega_1^2)}, \tag{70d}$$

and therefore Eq. (69) takes the form

$$\left[(k_\perp r_c)^4 + 2(k_\perp r_c)^2(k_y r_c)^2\frac{\omega_p^2}{\Omega_1^2}\right] = \frac{(\omega_D^2-4\Omega_1^2)}{3\Omega^2\omega_p^2}\left((k_\perp r_c)^2(\omega_D^2-\Omega^2) - (k_y r_c)^2\frac{\omega_p^4}{\Omega_1^2}\right), \tag{71}$$

where $k_\perp^2 = k_x^2 + k_y^2$. Without the small terms (proportional to ω_p^2/Ω^2 on both sides) Eq. (71) is the same as Eq. (61) (with $k_\perp^2$ replacing k_x^2) and predicts Bernstein modes propagating below $\omega = \Omega$ and above $\omega = 2\Omega_1(x)$. The last terms on either side of Eq. (71) represent the symmetry breaking effect caused by the gradient in the equilibrium electric field.

As in Sec. VI (a), for a fixed value of k_y, the plasma response is enhanced for quantized values of the driver frequency ω for which the waves have nodes at the antennae. Since waves with finite k_y sample the plasma drift which is an odd function of x, they do not have a definite parity.

(ii) r_c/L effect: Equations (31) and (34), which include the lowest-order r_c/L corrections for ν and v_d, are used in evaluating the expressions (49). Since

$$\omega_1 \simeq \omega_D + k_y(\omega_p^2/\Omega_1^2)(v_y - v_D), \tag{72a}$$

$$\omega_1 \mp \nu \simeq (\omega_D \mp \Omega_1) + \left(k_y\frac{\omega_p^2}{\Omega_1^2} \pm \frac{1}{2\Omega_1^2}\frac{d\omega_p^2}{dx}\right)(v_y - v_D), \tag{72b}$$

and

$$\frac{\partial f_0}{\partial v_y} = -\frac{m}{T_y}(v_y - v_D)f_0, \tag{73}$$

nonzero r_c/L corrections modify Eq. (51) into

$$\begin{aligned}
&\frac{d}{dx}\left(\left\{1 + \frac{\omega_p^2}{2\Omega_1}\left[\frac{1}{\Delta_-}Z\left(\frac{\omega_D-\Omega_1}{\Delta_-}\right) - \frac{1}{\Delta_+}Z\left(\frac{\omega_D+\Omega_1}{\Delta_+}\right)\right]\right\}\frac{d\phi_1}{dx}\right) \\
&\quad - k_y^2\left\{1 + \frac{\omega_p^4}{\Omega_1^2\Delta_0^2}Z'\left(\frac{\omega_D}{\Delta_0}\right) - \frac{\omega_p^2\Omega^2}{2\Omega_1^3}\left[\frac{(\omega_D-\Omega_1)}{\Delta_-^2}Z'\left(\frac{\omega_D-\Omega_1}{\Delta_-}\right) - \frac{(\omega_D+\Omega_1)}{\Delta_+^2}Z'\left(\frac{\omega_D+\Omega_1}{\Delta_+}\right)\right]\right\}\phi_1 \\
&\quad - k_y\phi_1\frac{d}{dx}\left\{\frac{\Omega\omega_p^2}{\Omega_1^2}\left[\frac{\omega_D}{\Delta_0^2}Z'\left(\frac{\omega_D}{\Delta_0}\right) - \frac{(\omega_D-\Omega_1)}{2\Delta_-^2}Z'\left(\frac{\omega_D-\Omega_1}{\Delta_-}\right) - \frac{(\omega_D+\Omega_1)}{2\Delta_+^2}Z'\left(\frac{\omega_D+\Omega_1}{\Delta_+}\right)\right]\right\} = 0,
\end{aligned} \tag{74}$$

where

$$\Delta_\pm = \left(\frac{2T_y}{m}\right)^{1/2}\left|k_y\frac{\omega_p^2}{\Omega_1^2} \mp \frac{1}{2\Omega_1^2}\frac{d\omega_p^2}{dx}\right| \tag{75a}$$

and

$$\Delta_0 = \left(\frac{2T_y}{m}\right)^{1/2}\left|k_y\frac{\omega_p^2}{\Omega_1^2}\right|. \tag{75b}$$

Again, the presence of the Z functions removes the singularities at $\omega_D = \Omega_1$ and $\omega_D = 0$ and gives rise to absorption of energy by particles at these layers.

VII. CONCLUSIONS

The response of a magnetized nonuniform plasma slab near the cyclotron frequency is significantly modified if the plasma is non-neutral. In the extreme non-neutral case of a single component plasma, the self-electric field of the plasma modifies the single particle gyrofrequency from the vacuum value $\Omega = qB_0/mc$ to a position-dependent value $\Omega_1(x) = [\Omega^2 - \omega_p^2(x)]^{1/2}$ providing an example of a collective plasma feature, the equilibrium electric field, affecting a fundamental single particle property, namely, the gyrofrequency.

A consequence of the modification of the value of the gyrofrequency from Ω to $\Omega_1(x)$ is that the upper hybrid resonance frequency is modified from the usual position-dependent value $[\Omega^2 + \omega_p^2(x)]^{1/2}$ to a constant value $[\Omega_1^2 + \omega_p^2]^{1/2} = \Omega$. Thus, with regard to position dependence, the roles of the single particle resonance and the collective resonance encountered in neutral plasmas are interchanged in a single component plasma.

In this work, starting from a self-consistent Vlasov equilibrium, the cold plasma response near the cyclotron frequency and the kinetic modifications to it are obtained from a systematic expansion of the integrodifferential equation satisfied by the wave potential solution of the linearized Vlasov–Poisson equations. One of the kinetic modifications is the introduction of a velocity dependence into the single particle gyration frequency $\Omega_1(x)$, leading to absorption of energy by particles at the resonant layers, where the frequency equals $\Omega_1(x)$. This absorption mechanism is present even when $k_z = 0$ (where k_z is the wavenumber parallel to the magnetic field) and when the magnetic field is strictly uniform. Another feature, uncovered by the kinetic theory, is the presence of thermal modes that are the analogs of Bernstein modes of neutral plasmas. A truncated second-order differential equation has been derived to describe these modes near the cyclotron frequency and the second harmonic, including the effects of $\mathbf{E}\times\mathbf{B}$ drift and diamagnetic drift. The equation predicts wave propagation for $\Omega_1 < \omega < \Omega$ and for $\omega > 2\Omega_1$. These modes can be driven by an external capacitor plate antenna and can reach large amplitudes at certain frequencies which are the magnetized non-neutral plasma analogs of Tonks–Dattner resonances.

ACKNOWLEDGMENT

This work was supported by the Office of Naval Research.

APPENDIX: EVALUATION OF $\int d\mathbf{v}\, u_y^m v_x^n f_0$

Integrals of the type $\int d\mathbf{v}\, u_y^m v_x^n f_0$, which are used in Sec. V in evaluating the orbit integral in Eq. (11), can be reduced to derivatives of the equilibrium density $n_0(x)$ multiplied by powers of $\bar{v}$. The equilibrium Vlasov equation, which has the form [see Eq. (44)]

$$-u_y \frac{\partial f_0}{\partial v_x} = v_x \left(\frac{1}{\Omega}\frac{\partial}{\partial x} - \frac{\partial}{\partial v_y}\right) f_0, \tag{A1}$$

is multiplied by $u_y^{m-1} v_x^{n+1}$ and integrated over velocity. Partial integrations over v_x on the left-hand side and over v_y on the right-hand side and a rearrangement of the x derivative yield

$$(n+1)\int d\mathbf{v}\, u_y^m v_x^n f_0 = \frac{1}{\Omega}\frac{d}{dx}\int d\mathbf{v}\, u_y^{m-1} v_x^{n+2} f_0 + (m-1)\frac{\Omega_1^2}{\Omega^2}\int d\mathbf{v}\, u_y^{m-2} v_x^{n+2} f_0, \tag{A2}$$

where the identity

$$\Omega^2 - \frac{q}{m}\frac{dE_0}{dx} = \Omega^2 - \omega_p^2 = \Omega_1^2(x)$$

has been used.

With repeated use of the transformation (A2), the right-hand side of (A2) can be expressed solely in terms of $\int d\mathbf{v}\, v_x^p f_0$ and its derivatives with respect to x. For f_0 given by Eq. (36), one obtains

$$\int d\mathbf{v}\, v_x^p f_0 = \begin{cases} [(p-1)(p-3)\cdots 3.1]\bar{v}^p n_0(x) & (p = \text{even}), \\ 0 & (p = \text{odd}). \end{cases}$$

Thus integrals of the type $\int d\mathbf{v}\, u_y^m v_x^n f_0$ can all be reduced to derivatives of $n_0(x)$ multiplied by powers of $\bar{v}$.

[1] G. A. Pearson, Phys. Fluids **9**, 2454 (1966); M. B. Chaudhury, T. Watanabe, and K. Nishikawa, J. Phys. Soc. Jpn. **51**, 3353 (1982).

[2] R. C. Davidson, *Theory of Nonneutral Plasmas* (Benjamin, Reading, MA, 1974).

[3] For a discussion of single particle orbits in non-neutral plasmas, see Sec. 1.2 of Ref. 1 and R. C. Davidson, in *Handbook of Plasma Physics* (North-Holland, Amsterdam, 1984), Vol. 2, Sec. 9.1.1. For a discussion of cold-fluid electrostatic waves in non-neutral plasmas, see Sec. 2.6 of Ref. 1 and R. C. Davidson, K. T. Tsang, and H. S. Uhm, Phys. Rev. A **32**, 1044 (1985).

[4] J. H. Malmberg and J. S. DeGrassie, Phys. Rev. Lett. **35**, 577 (1975).

[5] Energy absorption requires $E_0''(x) \neq 0$ and is absent in a kinetic description with a constant electric field [e.g., R. C. Davidson and H. S. Uhm, Phys. Fluids **21**, 60 (1978)] or a linearly increasing electric field (e.g., G. A. Pearson, Ref. 1).

[6] For a list of references on analogous finite Larmor radius expansions in neutral plasma drift waves, see N. A. Krall, in *Advances in Plasma Physics*, edited by A. Simon and W. B. Thompson (Wiley, New York, 1968), Vol. 1, p. 153.

[7] L. D. Landau and E. M. Lifshitz, *Mechanics* (Pergamon, Oxford, 1976), 3rd ed., p. 86.

[8] Reference 2, Sec. 3.7.

[9] L. Tonks, Phys. Rev. **37**, 1458 (1931); A. Dattner, Ericsson Tech. **2**, 309 (1957). For a more complete list of references, see J. V. Parker, J. C. Nickel, and R. W. Gould, Phys. Fluids **7**, 1489 (1964).

[10] B. D. Fried and S. C. Conte, *The Plasma Dispersion Function* (Academic, New York, 1961).